Topological susceptibility of Yang-Mills center projection vortices

R. Bertle

Atominstitut der Österreichischen Universitäten, Arbeitsgruppe Kernphysik, TU Wien, Austria

M. Engelhardt

Institut für Theoretische Physik, Universität Tübingen, Germany

M. Faber

Atominstitut der Österreichischen Universitäten, Arbeitsgruppe Kernphysik, TU Wien, Austria

The topological susceptibility induced by center projection vortices extracted from $SU(2)$ lattice Yang-Mills configurations via the maximal center gauge is measured. Two different smoothing procedures, designed to eliminate spurious ultraviolet fluctuations of these vortices before evaluating the topological charge, are explored. They result in consistent estimates of the topological susceptibility carried by the physical thick vortices characterizing the Yang-Mills vacuum in the vortex picture. This susceptibility is comparable to the one obtained from the full lattice Yang-Mills configurations. The topological properties of the $SU(2)$ Yang-Mills vacuum can thus be accounted for in terms of its vortex content.

I. INTRODUCTION

The center vortex picture of the Yang-Mills vacuum has recently experienced rapid development. Two advances figure prominently in particular. On the one hand, methods have been constructed with which it is possible to extract vortices from lattice gauge configurations; on the other hand, it has been realized that the vortex picture not only can account for confinement, but also for the topological properties of the Yang-Mills field.

In more detail, center vortices can be extracted from lattice gauge configurations using a combined gauge fixing and projection procedure. The first such procedure was presented in [1–3]; it involves fixing the gauge up to transformations from the center of the gauge group, by demanding maximization of a gauge fixing functional,

$$\max_{G} \sum_{i} |\mathrm{tr}\, U_i^G|^2 \qquad (1)$$

under gauge transformations G, where the U_i are the link variables specifying a lattice gauge configuration. This is called the (direct) maximal center gauge. It biases link variables towards the center of the gauge group, e.g. in the $SU(2)$ case considered henceforth, towards the elements ± 1. Physically, the idea is to transform as much physical information as possible to the center part of the configuration, i.e. the part one obtains by subsequently projecting

$$U \rightarrow \mathrm{sgn}\, \mathrm{tr}\, U. \qquad (2)$$

This projection step truncates physical information, and whether one has succeeded in retaining the relevant physics can usually only be answered *a posteriori*, by comparing the results obtained for a particular observable using either the center projected configurations or the full ones. If the results agree, this is called *center dominance*.

The observation of center dominance for large Wilson loops[1] [1–3] sparked the recent renewed interest in the *center vortex picture* of confinement. Once one has defined a $Z(2)$ lattice configuration by the center projection step (2), one equivalently obtains an associated center vortex configuration in a canonical fashion: One considers all plaquettes of the $Z(2)$ lattice, and if the product of the links bounding a plaquette yields the value -1, a vortex is defined to pierce that plaquette. These vortices form closed two-dimensional world-sheets in four-dimensional (Euclidean) space-time, and they can be thought of as being composed of plaquettes on the dual lattice, i.e. the lattice shifted by half a lattice spacing in all four directions with respect to the original one. Vortices contribute a phase factor -1 to the value of any Wilson loop they are linked to. Center dominance equivalently implies vortex dominance.

Depending on the observable under consideration, the original or the dual lattice (vortex) language may be advantageous. Note that, while the formulation in terms of $Z(2)$ link variables still has a residual $Z(2)$ gauge invariance [the gauge fixing functional (1) contains no bias with respect to transformations $G \in Z(2)$], the vortex world-sheets on the other hand represent gauge-invariant variables under this residual gauge group. One advantage of the vortex language lies in the fact that it can be detached from an underlying space-time lattice; one can consider vortex world-surfaces in continuous space-time. This has proven particularly useful when considering the topological properties of vortex configurations, which initially are only defined in a continuum framework [7–9]. The topological winding number (Pontryagin index) Q of an $SU(2)$ vortex surface configuration S can be given in terms of its (oriented) self-intersection number [7]

---

[1]This observation was subsequently extended to finite temperatures [4–6].

$$Q = -\frac{1}{16}\epsilon_{\mu\nu\alpha\beta}\int_S d^2\sigma_{\alpha\beta}\int_S d^2\sigma'_{\mu\nu}\delta^4(\bar{x}(\sigma)-\bar{x}(\sigma')) \quad (3)$$

where $\bar{x}(\sigma)$ denotes a parametrization of the two-dimensional surface S in four space-time dimensions, i.e. for any two-vector σ from a two-dimensional parameter space, the four-vector $\bar{x}$ gives the corresponding point on the vortex surface in space-time. This parametrization furthermore implies an infinitesimal surface element

$$d^2\sigma_{\mu\nu} = \epsilon_{ab}\frac{\partial\bar{x}_\mu}{\partial\sigma_a}\frac{\partial\bar{x}_\nu}{\partial\sigma_b}d^2\sigma \quad (4)$$

on the vortex surface. Note that the continuum surfaces thus must be specified not only with a location, but also an orientation, encoded in the sign of the surface element (4). In general, vortex surfaces consist of surface patches of alternating orientation; indeed, generic center projection vortices in the confining phase have been shown to be non-orientable [6], and therefore necessarily contain lines at which the orientation switches, i.e. patch boundaries. These lines can be associated with Abelian monopole trajectories[2] [7]. For $Z(2)$ lattice vortices, by contrast, the orientation information is initially lost and must be reintroduced before the topological charge can be evaluated [10]. Note furthermore that Eq. (3) includes not only surface self-intersections in the usual sense [for which Eq. (3) is normalized such as to give a contribution of modulus 1/2, as shown in [7,9]], but all singular points of a surface [10]; these are all points where the set of tangent vectors to the surface spans all four space-time directions.

The continuum expression (3) for the topological charge has been implemented for vortex surfaces defined on a (dual) space-time lattice [10]; the detailed prescription is presented in Sec. II. Using this construction, a random vortex surface ensemble defined such as to reproduce the confinement properties of $SU(2)$ Yang-Mills theory [11] was shown to simultaneously predict the correct topological susceptibility [10] as measured in lattice Yang-Mills experiments. The topological susceptibility $\chi = \langle Q^2\rangle/V$, where V is the space-time volume under consideration, e.g. determines, via the Witten-Veneziano estimate [12]

$$m_{\eta'}^2 + m_\eta^2 - 2m_K^2 = 2N_f\chi/f_\pi^2 \quad (5)$$

the anomalously high mass of the η' meson. These developments have given rise to the expectation that the vortex picture may be the first infrared effective framework capable of providing a consistent explanation of the entire spectrum of nonperturbative effects characterizing the infrared sector of Yang-Mills theory. Originally, the vortex picture was only proposed in particular to explain confinement [13]. It received early corroboration through the observation that a constant Yang-Mills chromomagnetic field is unstable with respect to the formation of flux tube domains in three-dimensional space [14]. Also in the lattice formulation, different possibilities of defining vortices were explored [15–17]. Notably, an alternative confinement criterion based on the vortex free energy was established [15] and measurements of this free energy have recently been carried out [18,19]. The new developments highlighted further above have significantly enlarged the scope of the vortex picture beyond this by establishing the link to the topological properties of Yang-Mills theory.

The purpose of the present work is to combine the two recent advances discussed above: The construction of the topological charge for lattice vortex surfaces [10], hitherto only applied to an ensemble of random vortex surfaces [10], will be used to measure the topological susceptibility associated with the vortices extracted from lattice Yang-Mills configurations via the maximal center gauge.[3] These vortex configurations exhibit ultraviolet artifacts which have been noted before in other contexts, cf. the discussion in Sec. III. These artifacts strongly influence the measurement of the topological charge, and it is consequently necessary to explore smoothing procedures applied to the vortices before the measurement. In this respect, the center projection framework is quite similar to full lattice Yang-Mills experiments. While the prediction for the topological susceptibility arrived at in this work is thus fraught with a measure of systematic uncertainty, the values obtained will be seen to be comparable with the full $SU(2)$ Yang-Mills topological susceptibility. This result is consistent with an interpretation of the topological charge of Yang-Mills configurations being generated by their vortex content.

Finally, a comment is in order regarding the gauge chosen to extract the vortices. The maximal center gauge to be used in the following has been the subject of recent debate due to pronounced Gribov copy effects. While most Gribov copies, i.e. local maxima of the gauge fixing functional (1), appear, as an ensemble, to generate center dominance for large Wilson loops, closer numerical scrutiny [21–24] has indicated that the highest maxima may not. This actually is not entirely surprising in view of the continuum limit of the maximal center gauge [7], which always leads to a trivial center projection, with no vortex content. One remedy suggested in [7] is to consider altered functionals,

---

[2]This becomes plausible if one invokes continuity of the *Abelian part* of the magnetic flux. A change in orientation of a vortex physically corresponds to an inversion of its magnetic flux, and thus implies the presence of a source or a sink of twice the (Abelian) magnetic flux of a vortex. This is precisely the flux emanating from or disappearing into an Abelian magnetic monopole or antimonopole. Correspondingly, one consistent possibility of defining the changes of orientation on the vortex surfaces lies in identifying them with the Abelian magnetic monopole world-lines detected in the maximal Abelian gauge, cf. also the more detailed comments at the beginning of Sec. II.

---

[3]Note that up to now only the complementary experiment has been performed [20]: An ensemble of Yang-Mills configurations from which all vortices had been removed was shown to belong exclusively to the topologically trivial sector $Q=0$.

$$\max_{G} \sum_{i} f(|\mathrm{tr}\, U_i^G|) \tag{6}$$

with monotonously rising f; any such functional implements the general idea of concentrating physical information onto the center of the gauge group. It is in fact quite straightforward to construct functions f which, in the continuum, avoid the singularities leading to the absence of vortices in the case of the gauge fixing functional (1). Another alternative type of gauge with which it is possible to identify vortices is the Laplacian center gauge [25–28], which is free of Gribov copies. While it is ultimately desirable to develop better-defined alternative gauge fixing procedures such as highlighted above, these procedures are just beginning to be explored.[4] For this reason, in this work, the usual maximal center gauge overrelaxation algorithm [1–3] will be used to *define* the gauge fixing image, in recognition of the fact that it does not strictly implement condition (1), cf. also the recent discussion in [30].

II. TOPOLOGICAL CHARGE OF LATTICE VORTEX SURFACES

Given vortex surface configurations composed of plaquettes on a (dual) hypercubic lattice, such as e.g. extracted via center projection from $SU(2)$ lattice Yang-Mills configurations, the Pontryagin index cannot immediately be evaluated. For one, as mentioned above, orientations first have to be assigned to the plaquettes making up the surface configuration. In the case of center projection vortices, one could use an indirect version of the maximal center gauge [1,2], in which one first transforms to the maximal Abelian gauge, extracts the Abelian monopoles via Abelian projection, and subsequently fixes the residual Abelian U(1) gauge freedom such as to reach the maximal center gauge. The monopoles define the edges of the oriented patches making up the vortex surfaces. However, this gauge fixing procedure does not perfectly locate the monopoles on the surfaces; there remains a small fraction of monopole links which do not lie on a vortex[5] [2]. In anticipation of the fact that the topological charge varies very little under most (topologically allowed) deformations of the monopole trajectories (the reason for this is discussed in detail in Sec. IV), in this work a simpler prescription was applied. Namely, vortex surfaces were identified by transforming directly to the maximal center gauge; then, random initial orientations were assigned to the vortex plaquettes, and sweeps through the lattice were performed in which plaquettes were reoriented such as to either maximize or minimize the monopole density. The to-

pological susceptibility was evaluated for both cases and turns out to be equal within the statistical error of the measurement, even though the monopole density varies by a large factor; numerical values are given in Sec. IV.

The oriented vortex surface configurations defined in this way contain two types of ambiguities as to their precise continuum interpretation, which must be resolved before the Pontryagin index can be evaluated. One ambiguity lies in the fact that the vortex surfaces generically intersect along whole lines, as opposed to points, as they do in the continuum. Similarly, monopole trajectories on the surfaces (at which the surface orientation switches) intersect singular points (at which topological charge is generated) with a finite probability; in the continuum, assuming a random distribution of lines and points on a surface, the two sets are generically disjoint. These ambiguities arise due to the coarse-graining enforced by the lattice; to resolve them, one defines the vortex configurations on a finer lattice and allows for random small deformations of the surfaces and of the monopoles until the ambiguities are resolved [10]. This is reminiscent of inverse blocking prescriptions in full Yang-Mills theory. In summary, one arrives at the following algorithm for evaluating the Pontryagin index of the lattice vortex surfaces (the reader interested in further details of the construction is referred to [10]).

(i) Transfer the given lattice surface configuration onto a lattice of 1/3 the lattice spacing and sweep once through the lattice, applying so-called elementary cube transformations whenever this leads to the removal of links along which two vortex surface segments intersect, i.e. to which more than two vortex plaquettes are attached. An elementary cube transformation[6] is a particular elementary update of a lattice surface configuration; it is carried out on all six plaquettes of an elementary three-dimensional cube of the lattice. If any of these plaquettes were part of a vortex before the update, then they are removed from the vortex after the update, and vice versa. Note that an elementary cube transformation preserves the closed character of the surfaces. The orientations of the updated plaquettes should be chosen such as to conserve the number of monopole links as much as possible. In practice, it is sufficient to carry this procedure out twice, i.e. one ends up with a lattice of 1/9 the original lattice spacing. As a result, the surface configuration only self-intersects at points, but not anymore along lines.

(ii) For each lattice site n, make a copy of all attached plaquettes, and transform the copy as follows. After finding an initial plaquette which is part of a vortex, iteratively re-orient further vortex plaquettes sharing links with previously considered ones such as to remove all monopole lines. If there are two independent surface segments present, i.e. two sets of vortex plaquettes which share only the lattice site under consideration, then carry out this procedure for each

---

[4]For some first results using the Laplacian center gauge, cf. [25–27,29]; note e.g. the as yet unclear interpretation of the vortex density in the Laplacian center gauge, which does not seem to scale properly with the renormalization group and seems to extrapolate to an infinite continuum value [29].

[5]In this respect, the Laplacian center gauge [25–28] is more advantageous, since it can be constructed such as to explicitly locate monopoles on vortex surfaces.

---

[6]Elementary cube transformations are also the basic building blocks of the smoothing procedure discussed in Sec. III B, albeit with a different acceptance criterion; Fig. 2 in Sec. III B displays particular examples of elementary cube transformations used in the context of smoothing.
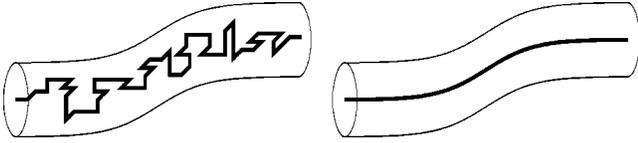
FIG. 1. Thick vortices (in a three-dimensional slice of space-time) associated with rough lattice center projection vortices (left), and smooth thin vortex cores (right), respectively.

segment independently. The result of this procedure is that all monopole lines are deformed away from the lattice site being scrutinized. Using the transformed vortex plaquettes, one can now obtain the contribution q_n to the Pontryagin index from the site n in question, cf. Eq. (3) and the discussion following. Namely, each pair of mutually orthogonal vortex plaquettes, i.e. with combined tangent vectors spanning four dimensions, contributes $\pm 1/32$ to the Pontryagin index. The sign depends on the relative orientation of the two plaquettes; the magnitude $1/32$ can be inferred from the fact that an intersection point in the usual sense contains 16 such pairs, and carries topological charge $q_n = \pm 1/2$, cf. [7,9].

(iii) The total Pontryagin index is the sum $Q = \Sigma_n q_n$.

Applying this procedure to general surface configurations on a hypercubic lattice, i.e. a space-time torus, one obtains a Pontryagin index quantized in half-integer units, which is exactly as it should be [31]; this is nontrivial in view of the fact that the magnitudes of the individual site contributions q_n can be as small as $1/16$ (for surfaces in a space-time continuum, the contribution from any particular singular point can even be arbitrarily small).

III. ELIMINATION OF ULTRAVIOLET ARTIFACTS

Using the above algorithm, the Pontryagin index of an arbitrary lattice center projection vortex configuration can be evaluated. However, such thin vortex surfaces exhibit ultraviolet artifacts which strongly contaminate the measurement. Specifically, in the vortex picture of Yang-Mills theory, thick physical vortices are conjectured to characterize the infrared properties of the vacuum. By contrast, the thin vortices obtained by center projection from full Yang-Mills configurations only approximate the aforementioned thick vortices on infrared length scales coarser than a scale related to the physical vortex thickness. On the other hand, within the thick profile of the physical vortex it corresponds to, the thin center projection vortex in general exhibits spurious gauge-dependent ultraviolet fluctuations, cf. Fig. 1.

This has been noted before in several contexts. For one, in [7] explicit examples were constructed showing that the precise location of a center projection vortex on scales finer than the physical vortex thickness depends on the gauge fixing function f in Eq. (6). Similarly, in [3] it was observed that this location varies as different Gribov copies of the maximal center gauge fixed configurations are considered. Moreover, in lattice experiments, the ratio between the string tension and the center projection vortex density is substantially suppressed compared to what one would expect from a random vortex ensemble [4]; motivated by this, the correlations between intersection points of center projection vortices with a

given space-time plane were investigated in [32]. On ultraviolet length scales, up to about 0.4 fm, the binary correlation function between these points indeed is strongly enhanced. Also this finding can be understood in terms of the aforementioned short wavelength fluctuations of the center projection vortices. Consider a plane which cuts a thick vortex, such as depicted in Fig. 1, along a (smeared-out) line, and consider furthermore intersection points of the associated center projection vortex with this plane. Due to the transverse fluctuations of the projection vortices, one will find a strongly enhanced probability of detecting such intersection points close to one another (compared with the probability one would expect from the mean vortex density). Note that this picture also clarifies the origin of the low ratio of the string tension to the center projection vortex density mentioned further above; the vortex density relevant for the area law behavior of the Wilson loop is the density of thick vortices, which would be well represented by smooth thin vortex cores, cf. Fig. 1, as opposed to the rough center projection vortices. Indeed, the smoothing procedure to be discussed in Sec. III B has been shown to keep the string tension approximately fixed while depleting the vortex density by eliminating ultraviolet fluctuations [6]; ultimately, one reaches a ratio compatible with the one expected in a random vortex ensemble.

As a consequence of these observations, it is necessary to explore methods to eliminate the spurious ultraviolet fluctuations of the center projection vortices; only then can one expect to extract the physical topological content of the configurations, without contamination by ultraviolet artifacts. Before discussing these methods, it is worth noting that the problems discussed above would be exacerbated by using the Laplacian center gauge instead of the maximal center gauge. In the latter, the center projection vortex density and its binary correlations measured in [32] scale properly under the renormalization group, such as to extrapolate to a finite physical result in the continuum limit, albeit with strong correlations in the ultraviolet, as discussed above. By contrast, it has recently been noted that in the Laplacian center gauge, the vortex density does not scale to a finite continuum limit, but appears to extrapolate to an infinite continuum density [29]. In a sense, the Laplacian center gauge may suffer from its own efficiency. As observed in [27], vortices extracted via the Laplacian center gauge at least partly reproduce the short-range Coulomb potential between static charges, whereas this effect is completely truncated when projecting from the maximal center gauge. In terms of the underlying degrees of freedom, this presumably means that, in addition to the infrared structure of the theory, Laplacian center gauge fixing attempts to also partially represent ultraviolet perturbative gluons by vortices. This may be the reason for the unphysical renormalization group behavior observed for the density of Laplacian center gauge vortices [29].

A. Blocking

A simple way to eliminate ultraviolet fluctuations of the center projection vortices obtained in the maximal center

gauge is to apply blocking steps such as to transfer the vortex configurations onto new coarser lattices, while always preserving their chromomagnetic flux content on length scales larger than the new lattice spacing. Such blocking steps are easily implemented starting on the original lattice, i.e. before constructing the vortex surfaces on the corresponding dual lattice.

Consider a new coarse lattice with n times[7] the spacing of an old fine lattice, superimposed on the latter such that all sites of the coarse lattice coincide with sites of the fine lattice. Then each link on the coarse lattice is defined to be equal to the product of the links on the fine lattice which make up the path of the coarse lattice link under consideration. Note that this implies that the gauge phases associated with plaquettes on the coarse lattice are equal to the $n \times n$ Wilson loops on the old fine lattice to which these plaquettes correspond; i.e., the chromomagnetic flux is preserved on scales as coarse as or coarser than the new lattice. Note furthermore that the following description of a blocking step is equivalent to the definition given above: If an odd number of vortices pierces the $n \times n$ Wilson loop on the old fine lattice, then one vortex pierces the corresponding plaquette on the new coarse lattice; if an even number of vortices pierces the $n \times n$ Wilson loop on the fine lattice, then no vortex pierces the corresponding plaquette on the coarse lattice. Note lastly that the coarse lattice is again a $Z(2)$ lattice; thus, vortex surfaces remain closed after blocking by construction.

In practice, the blocking procedure (and also the smoothing procedure discussed further below) was applied to the center projected lattice configurations *before* defining the orientations of the vortex surfaces in the manner described at the beginning of Sec. II. It should also be mentioned that blocking manifestly preserves the values of all Wilson loops (as far as they can still be defined on the coarse lattice). Thus, blocking leaves the string tension induced by a thin vortex ensemble invariant.

In Sec. IV, the behavior of the topological susceptibility as a function of the coarse lattice spacing reached by blocking is discussed. Of course, the question arises which scale defines the separation between spurious ultraviolet fluctuations to be eliminated, and relevant infrared information on vortex degrees of freedom to be kept. Obviously, this scale is related to the thickness of the physical vortices thought to be present in the full Yang-Mills configurations; however, the precise relation is *a priori* unclear. Certainly, the blocking procedure should not be carried so far as to deplete the density of thick vortices relevant for the asymptotic string tension. An estimate of this density, discussed in [33], leads to the conclusion that the centers of neighboring thick vortices, on the average, are 0.6 fm apart. This therefore constitutes an upper bound on the length scales to be eliminated by the blocking procedure. On the other hand, the ultraviolet correlations measured in [32], interpreted above to be a consequence of the spurious short wavelength fluctuations of the center projection vortex surfaces, extend to distances up to about 0.4
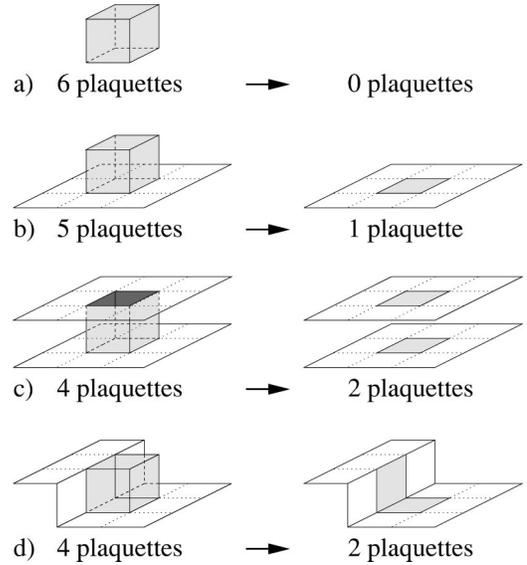

FIG. 2. Different smoothing steps effected by elementary cube transformations. They are distinguished by the number of vortex plaquettes removed and created by the operation. Note that two possibilities (c) and (d) of removing four plaquettes and creating two other ones are possible, depending on whether the latter two are opposite (c) or adjacent faces (d) of the elementary cube. The ordering of the steps (c) and (d) may at first sight seem counterintuitive, since (d) can be clearly visualized as smoothing the vortex surface, whereas (c) seems more severe and does not constitute a smoothing step in the strict sense; it can change the connectivity of the vortex world-sheets. The reason (c) is nevertheless carried out before (d) lies in the fact that including (c) in the smoothing procedure in practice has little effect on the observables measured here, while step (d) is the chief source of changes in the infrared properties of the surface ensemble, cf. Fig. 3. The weak effect of step (c) is due to the fact that instances where (c) is applied are rather rare.

fm. Thus, the authors estimate that the separation scale, i.e. the new lattice spacing which should be reached by blocking, roughly lies between 0.4 fm and 0.6 fm. This is also compatible with the findings in a random vortex surface model [11] adjusted to reproduce the confinement properties of $SU(2)$ Yang-Mills theory; there, two neighboring vortices can be identified as distinct down to a minimal distance of 0.4 fm.

It should be emphasized that the above estimates do not exclude the chromomagnetic flux of the vortices being smeared out considerably further; i.e., the flux of neighboring thick physical vortices may to a certain extent overlap [33]. The flux of a physical vortex has been argued to extend transversally over a distance of a little over 1 fm [3,34], in order to account e.g. for the Casimir scaling behavior of adjoint representation Wilson loops [35].

B. Smoothing

Another way to remove the artificial ultraviolet fluctuations of the center projection vortices is the smoothing procedure first discussed in [6]. It operates using elementary

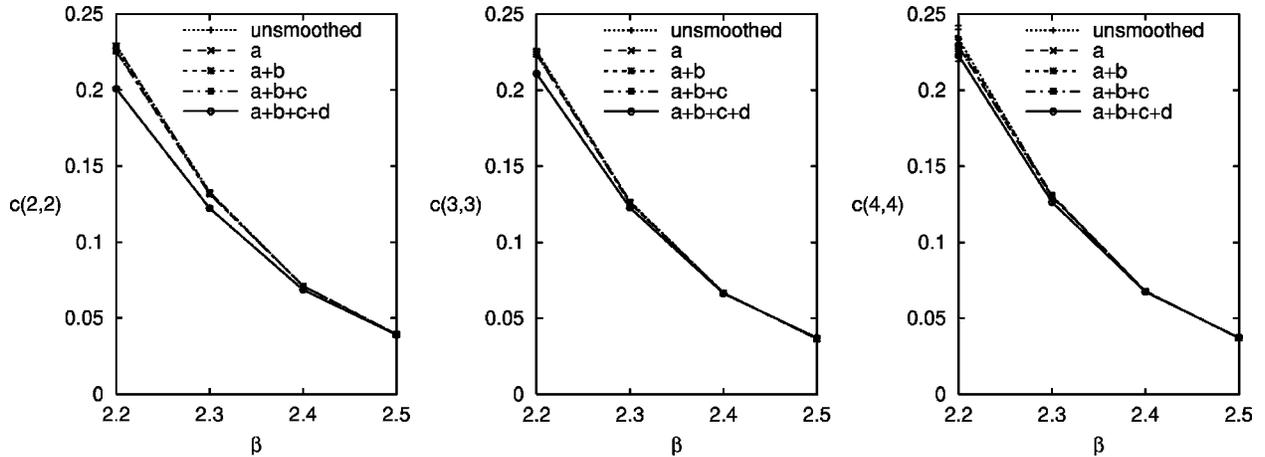---

[7]In practice, $n=2,3$ and 4 were used.

FIG. 3. Creutz ratios $c(2,2)$, $c(3,3)$ and $c(4,4)$ as a function of the inverse coupling β, for different versions of smoothing. Incorporating smoothing steps (a) through (c), cf. Fig. 2, leads to no appreciable change in the Creutz ratios compared with the unsmoothed ensemble. Only smoothing step (d) has a non-negligible effect on the static quark potential.

cube transformations of the type already introduced in Sec. II in connection with the removal of topological ambiguities in the lattice vortex surface configurations. The difference lies in the condition for accepting an elementary cube transformation. The smoothing procedure is defined by accepting such an elementary update whenever it implies a net decrease in the number of vortex plaquettes, and it can be further split up into a progression of steps characterized by the precise way in which the update affects the vortex surface, as displayed in Fig. 2. Note also that repeated smoothing sweeps through the lattice are performed, until no further elementary cube transformations of the type under consideration are possible; thus, smoothing can propagate information over distances of more than one lattice spacing.

This smoothing procedure depletes the center projection vortex density while keeping the long-range static quark potential largely intact, in accordance with the interpretation of the center projection vortices discussed above in connection with Fig. 1. However, in contrast to the blocking procedure presented in the previous section, preservation of the string tension is not an exact property of smoothing. Thus, invariance of the static potential can be used as a criterion to determine how far the smoothing procedure can be applied before it begins to truncate relevant physical information about the confining thick vortex structures, and should therefore be stopped.

The effect of the different smoothing steps on Creutz ratios is displayed in Fig. 3. The Creutz ratios are clearly unaffected by the smoothing steps (a) through (c), whereas a suppression is seen after step (d). At first sight, therefore, steps (a) through (c) only remove spurious ultraviolet fluctuations from the vortex configurations, whereas step (d) begins to truncate relevant information. However, two trends are visible in Fig. 3 which deserve further comment. For one, the suppression effect becomes weaker as one progresses to larger Wilson loops. This is natural; a finite number of local smoothing steps, which propagates information over a finite distance, cannot influence correlations on scales larger than

that distance.[8] Thus, strictly speaking, the asymptotic string tension is not modified by smoothing. However, already the medium range behavior of the confining static quark potential constitutes relevant nonperturbative information, e.g. through its influence on hadronic properties. In this sense, smoothing step (d) does truncate important nonperturbative effects carried by the vortices.

On the other hand, according to Fig. 3, the suppression of the Creutz ratios by smoothing step (d) also weakens as the inverse coupling β is increased. This can be understood from the fact that smoothing is not defined in a renormalization group invariant manner. Elementary smoothing operations are defined locally on the scale of one lattice spacing; as one increases β, this spacing decreases. Therefore, some fluctuations of the vortex surfaces which occur on the scale of one lattice spacing at low β (and are therefore removed by smoothing) remain unaffected by smoothing at higher β because they then extend over more than one lattice spacing.[9] The trend visible in Fig. 3 suggests that, at $\beta = 2.5$, one roughly reaches the point where smoothing step (d) just stops truncating relevant physical information (and, presumably, still removes spurious ultraviolet fluctuations). At higher β, smoothing step (d) can be expected to even leave some of these ultraviolet fluctuations intact.

As a consequence of the above discussion, the authors conclude that, at $\beta = 2.3$, the topological susceptibility measured from center projection vortices before applying smoothing step (d) constitutes an upper limit on the physical susceptibility carried by the confining thick physical vortices characterizing infrared Yang-Mills theory; the measurement after smoothing step (d) constitutes a lower limit. At $\beta = 2.5$, on the other hand, the value measured after smoothing

---

[8]Note that an analogous argument applies with regard to cooling steps applied to lattice Yang-Mills configurations.

[9]Renormalization group invariance would presumably be restored by considering smoothing steps of increasingly nonlocal nature as β is augmented.

step (d) should give a rough indication of the aforementioned relevant physical thick vortex susceptibility. It will be seen that these characterizations at different β are consistent with each other.

IV. NUMERICAL MEASUREMENTS AND DISCUSSION

Having presented all the elements employed in the analysis, the complete procedure used to extract the topological susceptibility can be summarized as follows.

(i) Generate an ensemble of $SU(2)$ lattice Yang-Mills configurations.

(ii) Transform the configurations to the maximal center gauge and perform center projection.

(iii) Remove ultraviolet fluctuations of the center projection vortex surfaces by either blocking or smoothing, cf. Sec. III.

(iv) Randomly assign orientations to the dual lattice plaquettes making up the surfaces, with a choice of bias which either maximizes or minimizes the monopole line density, cf. the beginning of Sec. II.

(v) Remove ambiguities in the vortex surfaces, i.e. lines along which vortices intersect and monopole lines coinciding with singular surface points, cf. Sec. II.

(vi) Evaluate the topological charge carried by the singular points, cf. Sec. II.

Numerical measurements were carried out for the coupling $\beta = 2.5$ on a 16^4 lattice, where 1156 samples were taken, and also for $\beta = 2.3$ both on a 16^4 lattice (1183 samples) and on a 12^4 lattice (4622 samples). Figure 4 depicts the results for the topological susceptibility χ of the different center projection vortex ensembles considered. Specifically, the fourth root of χ is given in units of the square root of the string tension σ, where the latter was simultaneously extracted from the center projected lattice ensemble (given center dominance [1–3], this is equivalent to using the string tension obtained from the full gauge configurations). Measurements are displayed as a function of the blocking scale (i.e. the spacing of the blocked lattice), and as a function of the smoothing steps. The fact that the $\beta = 2.3$ and the $\beta = 2.5$ values in the right-hand panel in Fig. 4 do not lie on a universal curve (as opposed to the left-hand panel) is natural, since the smoothing steps defining the horizontal axis are not constructed in a renormalization group invariant manner, cf. the discussion in the previous section.

The vertical error bars in Fig. 4 are compounded from two sources, namely the statistical uncertainty of the susceptibility measurement and the statistical uncertainty of the string tension measurement. The latter uncertainty in addition leads to the horizontal error bars displayed in the left-hand panel in Fig. 4, since the evaluation of σa^2 was also used to determine the lattice spacing a by equating $\sqrt{\sigma} = 440$ MeV.

It should be noted that, in addition to the purely statistical error bars displayed, there is a systematical uncertainty inherent in the determination of the topological susceptibility due to the necessity of applying the vortex surface ambiguity removal procedure discussed in Sec. II. This uncertainty is difficult to quantify. Some confidence in the reliability of the final results for the topological susceptibility can be derived

from the fact that the parallel use of two fundamentally distinct algorithms at intermediate stages, namely blocking and smoothing,[10] nevertheless leads to consistent estimates of the susceptibility, as will be seen further below.

Before proceeding to interpret Fig. 4, a discussion of the monopole density dependence of the results is in order. The measurements displayed in Fig. 4 were obtained using the maximal monopole density reached via the biased vortex plaquette reorientation procedure described at the beginning of Sec. II. If one conversely minimizes the monopole density, the values shown in Fig. 4 only change by at most 1%, i.e. by considerably less than the uncertainty of the measurement. Thus, for practical purposes, the topological susceptibility is independent of variations of the monopole density.[11] To illustrate the significance of this result, Fig. 5 displays the aforementioned maximal and minimal monopole line densities considered for each measured data point in Fig. 4. For comparison, the zero-temperature monopole line density measured in full $SU(2)$ Yang-Mills theory in the maximal Abelian gauge [36] amounts to $\rho_{mag} = 64/\text{fm}^3$.

The phenomenon that the topological susceptibility is independent of the monopole density has been observed before in the random vortex surface model [10]. Also the reasons for this independence there and here are similar. Most impor-

---

[10] The differences between the two algorithms in particular manifest themselves in the fact that, after blocking, a much larger amount of vortex surface ambiguity removal is necessary than after smoothing. Presumably, a coarse lattice, such as the surface configurations are forced onto by blocking, does not allow the vortices to avoid one another, thereby inducing a large density of lines on which vortex surfaces intersect. These ambiguities subsequently have to be removed again by correspondingly abundant applications of elementary cube transformations, as described in Sec. II. In the case of smoothing, much less alteration of the surfaces is needed. In this sense, smoothing seems to constitute a better preconditioner as far as the vortex surface ambiguity removal procedure is concerned. This difference between the algorithms becomes more and more pronounced with progressive blocking/smoothing, and it is to be expected that systematical influences of the vortex surface ambiguity removal on the topological charge affect the blocking results to a much greater degree than the smoothing results, thus directly manifesting themselves in a difference between these results. Nevertheless, the final estimates for the topological susceptibility obtained using the two procedures will be seen to be consistent with one another.

[11] It should be emphasized that this does not mean that the topological charge *exists* independent of the presence of monopoles. Indeed, oriented vortex configurations, i.e. those with no monopoles, carry vanishing Pontryagin index [7]. Rather, the nonorientability of the vortex surfaces implies a certain irreducible minimal monopole density, and the topological susceptibility is merely independent of changes in the monopole density implied by topologically trivial fluctuations of the monopoles, i.e. deformations which are topologically allowed while keeping the monopoles located on the vortex surfaces. Correspondingly, the topological charge can thus be evaluated without *explicit* knowledge of the monopoles. The relevant information is already encoded in the nonorientable character of the vortex surfaces.
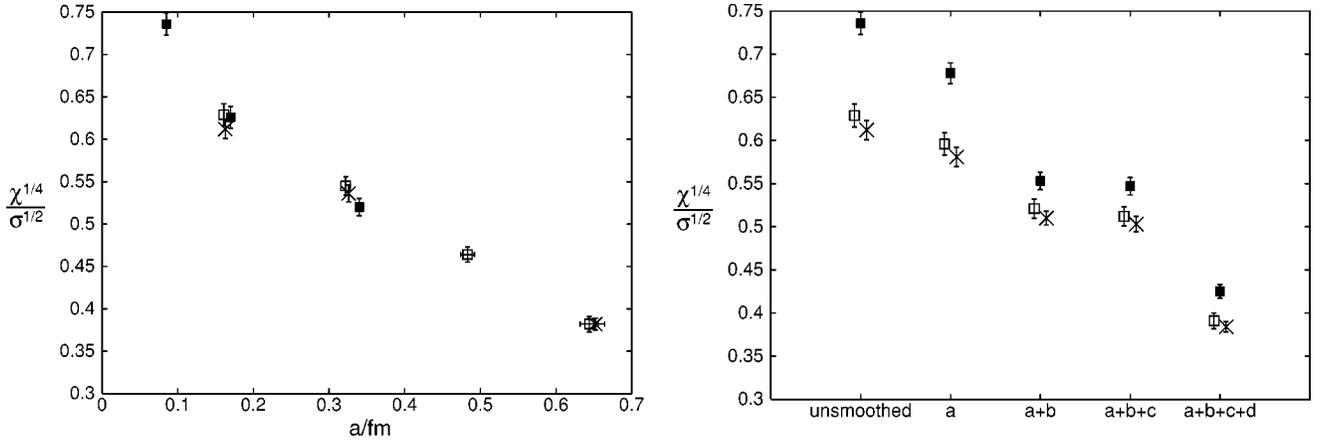
FIG. 4. Fourth root of the topological susceptibility χ carried by center projection vortices, in units of the square root of the string tension σ. Measurements are shown as a function of the blocking scale a (left) and of the smoothing steps (right). Open squares correspond to $\beta = 2.3$ on a 12^4 lattice, crosses to $\beta = 2.3$ on a 16^4 lattice, and filled squares to $\beta = 2.5$ on a 16^4 lattice. Error bars are discussed in the main text.

tantly, the dominant proportion of the topological charge is carried by so-called writhing points of the vortex surfaces as opposed to intersection points in the usual sense. The former class of singular points is distinguished from the latter as follows: At intersection points, two distinct surface segments share one point, but one cannot reach one surface segment from the other by proceeding along plaquettes which share a link. Writhing points on the other hand are characterized precisely by the opposite; all plaquettes attached to such a point can be connected by proceeding along plaquettes which share a link. In this sense, there is only one surface segment

at a writhing point. As a consequence of this structure, the associated contribution to the Pontryagin index is manifestly invariant under changes of the monopole configuration: Encircling a writhing point by a monopole loop implies inverting the orientations of all plaquettes attached to the point, since they are all connected via links. As a result, all pairs of orthogonal plaquettes retain their relative orientation, and the Pontryagin index is unchanged [10].

The topological susceptibility therefore must be independent of the monopole density to the extent that it is dominated by the contributions from writhing points. To corrobo-
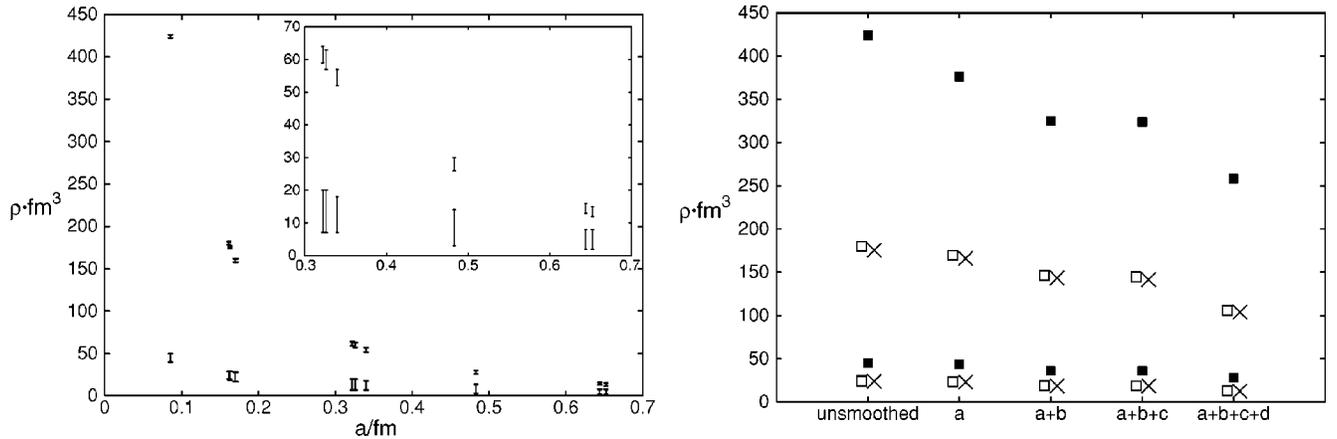

FIG. 5. Monopole line density ρ as a function of the blocking scale (left) and of the smoothing step (right). For each point on the horizontal axes, both the maximal and the minimal densities reached by the vortex plaquette reorientation procedure of Sec. II are shown, where in the right-hand panel, open squares correspond to $\beta = 2.3$ on a 12^4 lattice, crosses to $\beta = 2.3$ on a 16^4 lattice, and filled squares to $\beta = 2.5$ on a 16^4 lattice. In the left-hand panel, identification of the different β values and lattices is foregone for the sake of legibility; they can however be inferred by comparing with Fig. 4 (left), since the ordering of the data in the blocking scale is identical. Instead, the data are represented by vertical bars to indicate the rise in the densities induced by the vortex surface ambiguity removal procedure of Sec. II. Thus, the lower end of each vertical bar gives the monopole density originally defined by the plaquette reorientation procedure, whereas the upper end of each bar represents the density after the subsequent ambiguity removal; this is therefore the density at which the Pontryagin index was ultimately measured. The inset is simply an enlargement of the range [0.3 fm,0.7 fm] in the blocking scale. In the case of smoothing (right), the variation of the monopole density through the vortex surface ambiguity removal is always smaller than the symbols displayed; in fact, in marked contrast to the case of blocking, this variation becomes negligible with progressive smoothing steps, cf. also the discussion of the systematic uncertainty of the topological susceptibility further above.
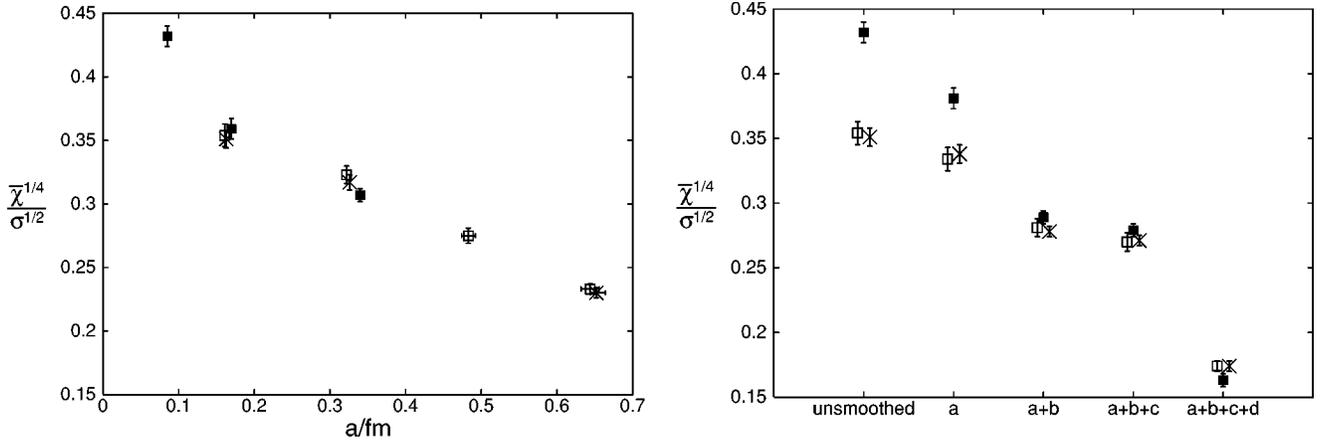
FIG. 6. Truncated topological susceptibility $\bar{\chi}$ of center projection vortices obtained by disregarding writhing points and taking only contributions from intersection points into account. For legibility, the fourth root of the susceptibility is displayed, in units of the square root of the string tension σ. Measurements are shown as a function of the blocking scale a (left) and of the smoothing steps (right). Open squares correspond to $\beta = 2.3$ on a 12^4 lattice, crosses to $\beta = 2.3$ on a 16^4 lattice, and filled squares to $\beta = 2.5$ on a 16^4 lattice.

rate this dominance, Fig. 6 displays the topological susceptibility $\bar{\chi}$ obtained by discarding writhing points (in all other respects, Fig. 6 is completely analogous to Fig. 4). Evidently, the fourth root of this truncated susceptibility is only roughly half as large as the fourth root of the full one; i.e., the contribution of intersection points to the full topological susceptibility is suppressed compared with the contribution from writhing points by roughly a factor 2^4.

Note furthermore that Fig. 6 was again obtained using the maximal monopole density reached via the biased vortex plaquette reorientation procedure of Sec. II. If one instead uses the minimal monopole density, the variation of the results in Fig. 6 still is rather weak; it amounts to no more than 5%, which is comparable to the statistical uncertainty of the measurement. This at first sight surprisingly weak dependence is presumably due to the high degree of non-orientability of the vortex surfaces. This non-orientability enforces a certain minimal monopole density which cannot be removed by the aforementioned vortex reorientation procedure. Evidently already this minimal density suffices to randomize the signs of the intersection point contributions to the Pontryagin index to such an extent that additional random changes of the signs, induced by adding monopole loops on the vortex surfaces, do not strongly influence the associated topological susceptibility.

The fact that the topological susceptibility is virtually independent of the monopole density allows to predict the former without going to the trouble of explicitly determining the monopole content of each lattice Yang-Mills configuration considered. The remaining task lies in extracting from Fig. 4 the physical value of the topological susceptibility obtained after eliminating spurious ultraviolet fluctuations of the center projection vortex surfaces.

Starting with the left-hand panel in Fig. 4, the discussion in Sec. III A led to the conclusion that the residual susceptibility χ at a blocking scale of 0.4 fm represents an upper limit for the physical susceptibility χ_{phys}, whereas the value at 0.6 fm constitutes a lower limit. In the extreme cases admitted by the error bars, this implies

$$(174 \text{ MeV})^4 \lesssim \chi_{phys} \lesssim (224 \text{ MeV})^4, \tag{7}$$

where $\sqrt{\sigma} = 440$ MeV was used. Likewise, in the right-hand panel in Fig. 4, the $\beta = 2.3$ data extracted using smoothing steps (a)–(c) limit the physical susceptibility from above, whereas the $\beta = 2.3$ data obtained using smoothing steps (a)–(d) limit it from below, cf. the discussion in Sec. III B. Therefore, one has in the extreme cases admitted by the error bars

$$(166 \text{ MeV})^4 \lesssim \chi_{phys} \lesssim (230 \text{ MeV})^4. \tag{8}$$

This is furthermore consistent with the value obtained at $\beta = 2.5$ using smoothing steps (a)–(d), namely $\chi^{1/4} = (187 \pm 3)$ MeV (only statistical error quoted).

In summary, the results for the topological susceptibility carried by the physical thick vortex content of lattice Yang-Mills configurations, as estimated within the different schemes of eliminating spurious ultraviolet fluctuations of the associated thin center projection vortices, are consistent with one another. While this agreement bolsters the confidence in the results obtained, it should be noted that the systematic uncertainties inherent in all the procedures used remain under limited control. A worthwhile possibility of achieving progress on this issue in the future lies in studying the correlation, configuration by configuration, between the topological charge extracted from the center projection vortices and the one determined from the original $SU(2)$ lattice Yang-Mills fields e.g. by cooling methods. Of course, also the latter methods are afflicted with a measure of uncertainty, and the outcome of the aforementioned detailed comparison would indeed be very interesting.

Keeping these caveats in mind, the range for the topological susceptibility carried by the center projection vortices obtained here corresponds well with values extracted from the full $SU(2)$ lattice Yang-Mills ensemble, cf. e.g. [37] and references therein. The latter values are located roughly at the center of the range admitted by Eqs. (7) and (8). This suggests that the topological properties of the Yang-Mills

ensemble can be accounted for in terms of the vortex content of the gauge field configurations, just as is the case for the confining properties. The vortex picture appears suited to provide a unified description of these two different nonperturbative aspects of Yang-Mills theory.

[1] L. Del Debbio, M. Faber, J. Greensite, and Š. Olejník, Phys. Rev. D **55**, 2298 (1997).

[2] L. Del Debbio, M. Faber, J. Greensite, and Š. Olejník, in *New Developments in Quantum Field Theory*, edited by P. H. Damgaard and J. Jurkiewicz (Plenum Press, New York, 1998); hep-lat/9708023.

[3] L. Del Debbio, M. Faber, J. Giedt, J. Greensite, and Š. Olejník, Phys. Rev. D **58**, 094501 (1998).

[4] K. Langfeld, O. Tennert, M. Engelhardt, and H. Reinhardt, Phys. Lett. B **452**, 301 (1999).

[5] M. Engelhardt, K. Langfeld, H. Reinhardt, and O. Tennert, Phys. Rev. D **61**, 054504 (2000).

[6] R. Bertle, M. Faber, J. Greensite, and Š. Olejník, J. High Energy Phys. **03**, 019 (1999).

[7] M. Engelhardt and H. Reinhardt, Nucl. Phys. **B567**, 249 (2000).

[8] J. M. Cornwall, Phys. Rev. D **58**, 105028 (1998).

[9] J. M. Cornwall, Phys. Rev. D **61**, 085012 (2000).

[10] M. Engelhardt, Nucl. Phys. **B585**, 614 (2000).

[11] M. Engelhardt and H. Reinhardt, Nucl. Phys. **B585**, 591 (2000).

[12] E. Witten, Nucl. Phys. **B156**, 269 (1979); G. Veneziano, *ibid.* **B159**, 213 (1979).

[13] G. 't Hooft, Nucl. Phys. **B138**, 1 (1978); Y. Aharonov, A. Casher, and S. Yankielowicz, *ibid.* **B146**, 256 (1978); J. M. Cornwall, *ibid.* **B157**, 392 (1979).

[14] H. B. Nielsen and P. Olesen, Nucl. Phys. **B160**, 380 (1979); J. Ambjørn and P. Olesen, *ibid.* **B170 [FS1]**, 60 (1980); **B170 [FS1]**, 265 (1980); P. Olesen, *ibid.* **B200 [FS4]**, 381 (1982).

[15] G. Mack and V. B. Petkova, Ann. Phys. (N.Y.) **123**, 442 (1979); G. Mack, Phys. Rev. Lett. **45**, 1378 (1980); G. Mack and V. B. Petkova, Ann. Phys. (N.Y.) **125**, 117 (1980); G. Mack, in *Recent Developments in Gauge Theories*, edited by G. 't Hooft *et al.* (Plenum, New York, 1980); G. Mack and E. Pietarinen, Nucl. Phys. **B205 [FS5]**, 141 (1982).

[16] E. T. Tomboulis, Phys. Rev. D **23**, 2371 (1981).

[17] A. Hart and M. Teper, Phys. Rev. D **60**, 114506 (1999).

[18] T. G. Kovács and E. T. Tomboulis, Phys. Rev. Lett. **85**, 704 (2000).

[19] A. Hart, B. Lucini, Z. Schram, and M. Teper, J. High Energy Phys. **06**, 040 (2000).

[20] P. de Forcrand and M. D'Elia, Phys. Rev. Lett. **82**, 4582 (1999).

[21] T. G. Kovács and E. T. Tomboulis, Phys. Lett. B **463**, 104 (1999).

[22] V. G. Bornyakov, D. A. Komarov, M. I. Polikarpov, and A. I. Veselov, JETP Lett. **71**, 231 (2000); hep-lat/0002017.

[23] R. Bertle, M. Faber, J. Greensite, and Š. Olejník, J. High Energy Phys. **10**, 007 (2000).

[24] V. G. Bornyakov, D. A. Komarov, and M. I. Polikarpov, Phys. Lett. B **497**, 151 (2001).

[25] C. Alexandrou, M. D'Elia, and P. de Forcrand, Nucl. Phys. B (Proc. Suppl.) **83**, 437 (2000).

[26] C. Alexandrou, P. de Forcrand, and M. D'Elia, Nucl. Phys. A **663**, 1031 (2000).

[27] P. de Forcrand and M. Pepe, Nucl. Phys. **B598**, 557 (2001).

[28] H. Reinhardt and T. Tok, hep-th/0009205; Phys. Lett. B **500**, 173 (2001).

[29] K. Langfeld, H. Reinhardt, and A. Schäfke, Phys. Lett. B **504**, 338 (2001).

[30] M. Faber, J. Greensite, and Š. Olejník, Phys. Rev. D **64**, 034511 (2001).

[31] G. 't Hooft, Nucl. Phys. **B153**, 141 (1979); P. van Baal, Commun. Math. Phys. **85**, 529 (1982); M. Garcfia Pérez, A. González-Arroyo, A. Montero, C. Pena, and P. van Baal, Nucl. Phys. B (Proc. Suppl.) **83**, 464 (2000).

[32] M. Engelhardt, K. Langfeld, H. Reinhardt, and O. Tennert, Phys. Lett. B **431**, 141 (1998).

[33] R. Bertle, M. Faber, J. Greensite, and Š. Olejník, Nucl. Phys. B (Proc. Suppl.) **94**, 482 (2001).

[34] M. Faber, J. Greensite, and Š. Olejník, J. High Energy Phys. **06**, 041 (2000).

[35] M. Faber, J. Greensite, and Š. Olejník, Phys. Rev. D **57**, 2603 (1998).

[36] V. G. Bornyakov, E. M. Ilgenfritz, M. L. Laursen, V. K. Mitryushkin, M. Müller-Preussker, A. J. van der Sijs, and A. M. Zadorozhnyi, Phys. Lett. B **261**, 116 (1991).

[37] I.-O. Stamatescu, hep-lat/0002005.